ACS SENSORS

Article

Cite This: ACS Sens. 2019, 4, 389−397

pubs.acs.org/acssensors

Halogen Bonding Interactions for Aromatic and Nonaromatic Explosive Detection

Arjun K. A. Jaini, Lillian B. Hughes, Michael M. Kitimet, Kevin John Ulep, Michael C. Leopold,* and Carol A. Parish*

Department of Chemistry, Gottwald Center for the Sciences, University of Richmond, Richmond, Virginia 23173, United States

Supporting Information

ABSTRACT: Improved sensing strategies are needed for facile, accurate, and rapid detection of aromatic and nonaromatic explosives. Density functional theory was used to evaluate the relative binding interaction energies between halogen-containing sensor model molecules and nitro-containing explosives. Interaction energies ranged from −18 to −14 kJ/mol and highly directional halogen bonding interactions were observed with bond distances ranging between 3.0 and 3.4 Å. In all geometry optimized structures, the sigma-hole of electropositive potential on the halogen aligned with a lone pair of electrons on the nitro-moiety of the explosive. The computational results predict that the strongest interactions will occur with iodine-based sensors as, of all the halogens studied, iodine is the largest, most polarizable halogen with the smallest electronegativity. Based on these promising proof-of-concept results, synthetically accessible sensors were designed using 1,4-dihalobenzene (X = Cl, Br, and I) with and without tetra-fluoro electron withdrawing groups attached to the benzene ring. These sensing molecules were embedded onto single walled carbon nanotubes that were mechanically abraded onto interdigitated array electrodes, and these were used to measure the responses to explosive model compounds cyclohexanone and dimethyl-dinitro-benzene in nitrogen gas. Amperometric current−time curves for selectors and control molecules, including concentration correlated signal enhancement, as well as response and recovery times, indicate selector responsiveness to these model compounds, with the largest response observed for iodo-substituted sensors.

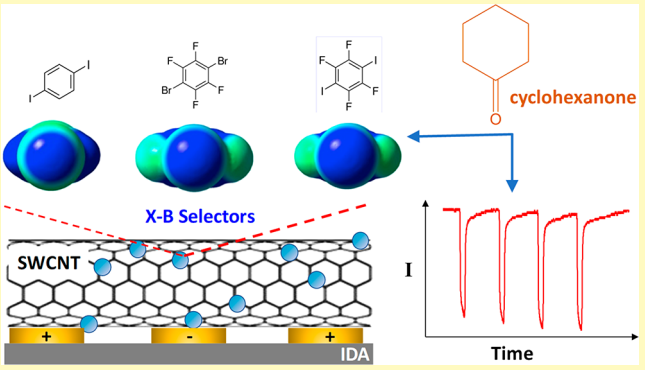

KEYWORDS: *explosive detection, halogen bonding, carbon nanotube-based sensor, chemiresistive, cyclohexanone*

The ability to quickly and accurately detect the presence of explosives is important to the field of security, national defense, and counter-terrorism efforts.[1] There are two main structural categories of explosives, aromatic compounds (e.g., 2,4,6-trinitroluene (TNT), 2,4-dinitrotoluene (2,4-DNT), and 2,6-dinitrotoluene (2,6-DNT)), and nonaromatic molecules (e.g., 1,3,5-trinitro-1,3,5-triazinane (RDX), 1,3,5,7-tetranitro-1,3,5,7-tetrazocane (HMX), pentaerythritol tetranitrate (PETN)), Figure 1a−f. While both categories possess a range of explosive power, nonaromatic explosives are more difficult to detect due to their low vapor pressure. The vapor pressure of RDX (~8.3×10^{-10} Torr), for example, is 4 orders of magnitude lower than the vapor pressure of TNT (~4.8×10^{-6} Torr).[1] The low vapor pressure of nonaromatic explosives cause these molecules to exhibit "stickiness" with various surfaces, making them attractive targets in the design of new devices targeting difficult-to-detect explosives. Similar to aromatic explosive molecules, the nonaromatic variety feature multiple, electron-rich NO_2 groups as a major structural component (Figure 1).

While direct detection of these compounds would be ideal, there are also other molecules that can be present within certain explosive materials that can be used as an indirect target for detection. In some cases, these compounds are byproducts of the primary explosive production process while, in other instances, they are more volatile molecules, known as detection taggants, purposely added to explosives by manufacturers to enable higher detectability of the explosive material. For example, it has been reported using headspace gas chromatography-mass spectrometry (GC-MS) analysis that volatile byproducts such as cyclohexanone (CH) (~1×10^{0} Torr) and 2-ethyl-hexanol (~1×10^{-1} Torr) are emitted during the synthesis and recrystallization of RDX, a component of untagged plastic explosives such as Composition 4 (C-4) and Semtex.[2] One of the more common components of tagged plastic explosives such as C-4 and Semtex, as well as Detasheet, which contains PETN, is the semivolatile (~1×10^{-3} Torr) taggant or marker compound dimethyl-dinitro-butane (DMNB).[2] Like their primary explosive counterparts, it is noteworthy that DMNB and CH (Figure 1g,h) feature nitro

Received: October 16, 2018
Accepted: January 23, 2019
Published: January 23, 2019

DOI: 10.1021/acssensors.8b01246
ACS Sens. 2019, 4, 389−397

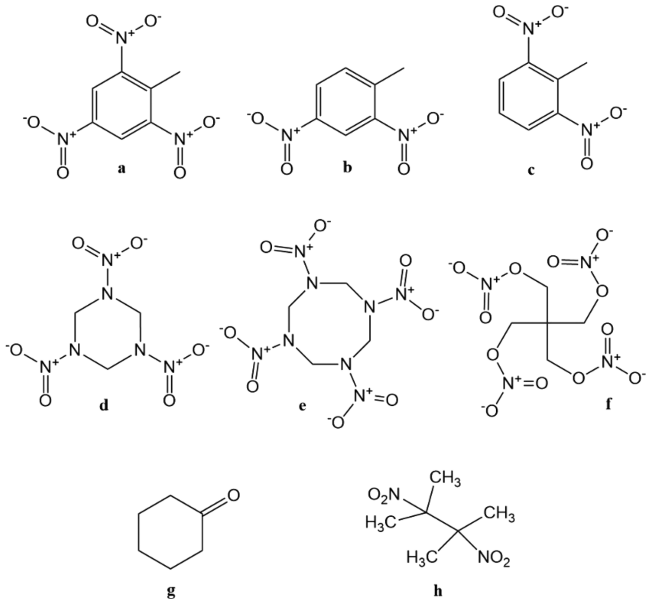

Figure 1. Aromatic explosive example molecules: (a) 2,4,6-trinitroluene (TNT), (b) 2,4-dinitrotoluene (2,4-DNT), and (c) 2,6-dinitrotoluene (2,6-DNT) and nonaromatic explosive example molecules: (d) 1,3,5-trinitro-1,3,5-triazinane (RDX), (e) 1,3,5,7-tetranitro-1,3,5,7-tetrazocane (HMX), and (f) pentaerythritol tetranitrate (PETN) as well as molecules.

groups, or electron-rich, lone-pair containing peripheral oxygen atoms, respectively. Collectively, the molecules shown in Figure 1 represent both direct and indirect target compounds for the development of sensors to effectively detect nearly imperceptible explosives.

A number of methods and materials are currently in use or are being developed to effectively detect explosive or explosive-related molecules with an emphasis of detecting trace amounts with high selectivity using smaller devices that are cost-effective. The need, approaches, and challenges are effectively detailed in a review by Thundat and Senesac.[1] Canine olfaction, one of the oldest and widely used explosive detection methods, has limitations in that the animals are extremely labor intensive in terms of training and care and can only be used for a few hours a day.[3] Interestingly, in the United States, canines are typically trained on detection of the taggant DMNB at 0.5 ppb, rather than the actual explosive molecule, making them less effective for detecting the presence of untagged plastic explosives.[4]

Ion mobility spectrometry (IMS) is another widely used explosive detection method, particularly at airports and security checkpoints, but is dependent on sample collection via surface swabbing prior to injection into the IMS.[5] While this method is effective for TNT in the picogram range, nonaromatic explosives are much more difficult to detect due to their low volatility and ability to easily adhere to surfaces.[5,6] There are also several inexpensive, noninstrumental explosive detection colorimetric assays, such as the Meisenheimer and Griess methods, that rapidly indicate the presence of nitrites and nitroaromatics as a presumptive gun-shot residue analysis,[7−9] though they lack specificity and are prone to false positives.[8]

Spectroscopic methods, measuring both fluorescence quenching[7,10−15] and activation,[16−19] have been successfully demonstrated to provide both mobile and sensitive detection of explosives or explosive-related molecules. These techniques have been used to detect low concentrations (ppm) of aromatic explosives such as TNT as well as nonaromatic explosives such as RDX and PETN. Fluorescence quenching during interactions of explosives with large, organic conjugated polymers has been incorporated into a commercialized, hand-held system known as Fluorescence Impersonating Dog Olfaction (FIDO). FIDO can detect aromatic TNT molecules in the ppb range and is effective for land mines and improvised explosive devices (IEDs).[20] The same research group demonstrated the use of fluorescence to capture nitroester and nitroamine moieties after photofragmentation of C4, successfully detecting nonaromatic RDX (1.2 ng) and PETN (0.320 ng).[16,21] While the fluorescent-based techniques[7,10−21] represent important progress toward effective explosive detection, the creation of new materials and strategies that can emphasize specific interactions between selector and target explosive molecules remain of high interest to easily and accurately detect a wider range of explosives or taggants.

Carbon nanotubes (CNTs), graphene sheets rolled into a tube, continue to be a highly investigated material as a functional component of chemical sensors for a variety of different targets, including explosive detection, and there are extensive literature reviews available.[22,23] The structural network of π-electrons found in CNTs creates an organic wire of significant length and high conductivity that is extremely sensitive to changes in the local environment, an attractive property for use in electrochemical or chemiresistive sensor designs.[24−26] In chemiresistive sensors, the conductance of the CNTs changes upon exposure to the target analyte. The suspected response mechanism is thought to be influenced by three types of interactions: intra-CNT interactions with the analyte, inter-CNT interactions with the analyte, and/or the interfacial electronic coupling of the CNTs with the electrode.[22] The specific architecture of the CNT material, the nature of the target analyte, and the electrode interface or modification thereof (i.e., Schottky barrier effects) can influence the relative impact of each of these interactions during transduction. Intra-CNT responses involve individual CNTs where analyte interaction disrupts the number or mobility of charge carrier holes within the material, such as the adsorption of e^- donating species that transfers charge and decreases hole conduction (i.e., increasing resistance). Inter-CNT interactions, either analyte partitioning between CNTs or within a coating on the CNT, can cause small changes in the space between CNTs (i.e., film swelling), exponentially increasing overall film resistance with separation distance. Effective selectivity continues to be a challenge for CNT-based sensors. While specificity for a single target species is usually difficult to attain with CNTs, significant selectivity has been achieved via CNT modification with coatings featuring selector molecules that are able to promote some discrimination against interferents.[22]

Halogen bonding (X−B) is a highly directional, noncovalent interaction between a region of positive electrostatic potential on a halogen atom and a Lewis base.[27] The region of positive electrostatic potential is created by the polarizability of a halogen atom bonded to electronegative groups that pull electron density from the halogen atom along the σ bond axis, leaving behind a positively charged area referred to as a "sigma hole."[28] X−B is even more directionally constrained than hydrogen bonding (H−B) due to the position of the sigma hole, which forms along the covalent bond of the halogen

DOI: 10.1021/acssensors.8b01246
ACS Sens. 2019, 4, 389−397

atom.[29] The sigma hole is highly tunable,[30] and its size mainly depends on the polarizability and electronegativity of the halogen atom and the strength of the electron withdrawing group connected to the halogen atom.[29,30] While X−B has been explored computationally, including small inorganic and organic molecular systems[31] as well as their potential contributions in DNA base pairing,[32] experimental evidence and application of X−B, particularly in combination with computational support, appear less often in the literature. Van der Boom and co-workers used halogen bonding interactions as the premise of noncovalent assembly of gold nanoparticles (NPs) onto planar surfaces.[33] Additionally, the unique X−B property of being an extremely linear, noncovalent interaction has useful applications in crystal engineering of novel structures,[34] and it has been reported that X−B is sometimes preferred to H−B in various solutions and crystal structures.[35,36] Recently, a combination experimental and computational study established evidence of X−B between astatine monoiodide and cyclohexane.[37] Additionally, the linear property of X−B has been used in various other electrochemical sensors that can detect specific anions.[38−42]

In this report, a combination of computational and experimental methods was used to explore the energetics of X−B bonding in model halogen-based molecules and Lewis bases, including NO_2 containing explosives and explosive-related molecules. Density functional theory was utilized to perform proof-of-concept calculations aimed at understanding the interactions of specific selector molecules (X−B donors) with both aromatic and nonaromatic explosives as well as key explosive-related taggants and byproducts. The calculations established the feasibility of using X−B as a functional component of an experimentally based, molecular recognition sensing strategy for explosives. Experimental design of a carbon nanotube (CNT) based sensor featuring the selector molecules successfully established expected X−B trends and the fast, concentration-dependent detection of targeted explosive-related molecules. To our knowledge, a study that combines both the computational and experimental evidence of X−B, specifically geared toward successful detection of the presence of nonaromatic explosive molecules, is currently not present in the literature.

EXPERIMENTAL DETAILS

Computational Methods. As a proof-of-concept, computational quantum chemistry was used to estimate the energy of interaction between various halogen based sensor molecules (X−B donors) and Lewis bases, including aromatic and nonaromatic explosives, as well as taggants, byproducts and carrier gases. Gas-phase geometry optimization of the halogen bonded complexes, sensor molecules, and Lewis bases was performed using the Gaussian09 software[43] utilizing Becke's hybrid B3LYP functional[44] with the cc-pVDZ basis sets.[45,46] For the larger halogens, iodine and bromine, the small (28-electron) Dirac−Fock (MDF) effective-core pseudopotentials and the corresponding basis sets were used.[47,48] Further computational details are provided in the Supporting Information.

Vapor Sensing Materials and Methods: Experimental Details. Sensor design fabrication and vapor testing were all modeled after procedures by Swager et al. 2015,[40,49] and are briefly described here with additional details provided in the Supporting Information. Interdigitated array (IDA) electrodes (gold on ceramic substrate; 2.2 cm × 7.6 cm × 0.7 cm with 200 μm band and gap widths) and their corresponding electronic connectors were obtained from DropSens (Metrohm). Pristine single-walled carbon nanotubes (p-SWCNTs) were purchased from NanoLab, Inc. (Waltham, MA) and modified with commercially available selector molecules using a ball-milling procedure.[40,49] The resulting material was mechanically compressed into a PENCIL (see the Supporting Information) with the resulting pellet mechanically abraded across a clean IDA until a film resistance of 0.1−3.0 kΩ was achieved, as determined from current−voltage measurements (0.1 to −0.1 V) recorded with a potentiostat (CH Instruments, model 630B).[50]

SWCNT-selector modified IDAs were inserted into an in-house built flow system (see Supporting Information) and allowed to equilibrate under a stream of nitrogen overnight prior to being quickly transferred to the Teflon cell holder, also under nitrogen flow, where they were allowed re-equilibrate under a constant applied potential (0.1 V, ≥ 500 s) to establish an initial, stable baseline current. Current through the sensors was monitored via amperometric current−time (I−t) curves while exposing the sensor to various concentrations of cyclohexanone with nitrogen as the carrier gas. Additional experimental details are provided in the Supporting Information.

RESULTS AND DISCUSSION

Determining the X−B Strength of Experimentally Accessible Selectors. Density functional theory was utilized to determine the strength of X−B interactions between a number of halogenated systems (X−B donors) and lone-pair containing Lewis base target molecules (X−B acceptors). The computational determination of stronger binding energies (E_{int}), shorter X−B bonds and linear interaction angles indicates X−B interactions that are more likely to be practically employed in experimental strategies targeting the same molecules.[30−32,51]

Dihalogen selector molecules featuring a halogen at the 1 and 4 positions of an aromatic ring were selected as the X−B partner, either with (strong X−B) or without (weak X−B) tetrafluoro electron-withdrawing functionality added to the aromatic ring (Figure 2A). The use of selectors containing dihalogen-substituted aromatic rings was appealing as they provide a mechanism for physically immobilizing the selector to CNTs while avoiding the complications that would arise from competing H−B interactions from hydroxyl and carboxylate substituted rings (results not shown). For each selector candidate, the halogen (X) was varied from iodine to bromine to chlorine with the expectation that X−B strengthens as one moves down Group VII and the halogen becomes more polarizable and less electronegative. For comparison, NH_3 was included in our calculations, along with the representative aromatic and nonaromatic explosives and explosive-related compounds CH and DMNB, the latter allowing for a safer work-flow in our experimental proof-of-concept study described below. NH_3 is a model analyte offering a lone pair of electrons for X−B. In our computational work, hexane served to model the behavior of the experimentally used control compound octadecane, structurally incapable of X−B interactions.

A major facet of X−B is its dependence on the halogen engaged in the interaction. For example, as illustrated in Figure 2B, there is a significantly larger sigma hole on the halogen in 1,4-diiodotetrafluorobenzene relative to 1,4-dichlorotetrafluorobenzene. The low electronegativity, high polarizability, and large percent s character of the unshared electrons on iodine, combined with the electron withdrawing properties of fluorine in the tetrafluorobenzene moiety, all contribute to a large sigma hole on iodine.[29] Accordingly, the E_{int} between 1,4-diiodotetrafluorobenzene and ammonia, a model X−B acceptor molecule, is significant at −37.18 kJ/mol (Table 1). For comparison, E_{int} for the H−B interaction in the water dimer is −21 kJ/mol (calculated with CCSD(T)/cc-aug-pVQZ),[52]

DOI: 10.1021/acssensors.8b01246
ACS Sens. 2019, 4, 389−397

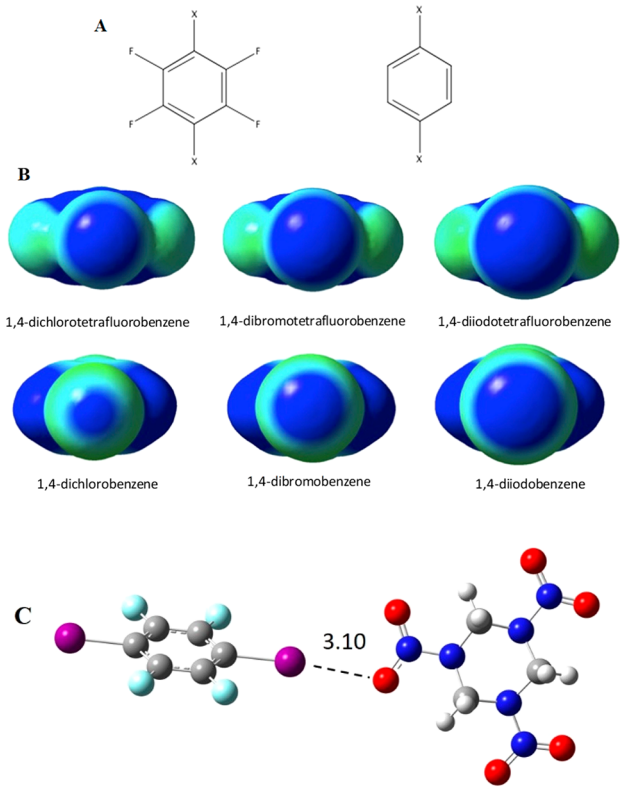

Figure 2. (A) 1,4-dihalogen aromatics either with or without additional 2,3,5,6-tetrafluoro substitution and where X varied from Cl to Br to I were studied as selector molecules; (B) sigma holes on 1,4-dichlorobenzene, 1,4-dibromobenzene, 1,4-diiodobenzene, 1,4-dichlorotetrafluorobenzene, 1,4-dibromotetrafluoro-benzene, and 1,4-diiodotetrafluorobenzene. This shows the increase in size of the sigma hole as EWGs are added to the aromatic ring and as the size and polarizability of the halogen increases. (C) Geometry optimized halogen bonded structure between RDX with 1,4-diiodotetrafluorobenzene. Bond lengths are shown in Å. The C−X−O bond angle is 174.9. Structures of all X−B complexes, showing the dependence of E_{int} on halogen, EWG, and resulting geometry can be found in the Supporting Information.

establishing that X−B can be a significant interaction, particularly if the structure of the interacting molecules are strategically chosen. We explored the binding interaction energies and complex geometries for many compounds (Table SI-1). The computational results for the interaction of our best selector 1,4-diiodotetrafluorobenzene with aromatic and nonaromatic explosive molecules as well as explosive-related taggants and byproduct molecules suggest significant interaction (Table 1).

With the 1,4-diiodotetrafluorobenzene selector, interaction energies for aromatic explosives (TNT, 2,4-DNT, and 2,6-DNT) range from −15.1 to −18.1 kJ/mol while the range for nonaromatics (RDX, HMX, and PETN) is −13.9 to −16.8 kJ/mol. The interaction energy for byproduct CH is −23.4 kJ/mol and for taggant DMNB it is −18.2 kJ/mol. For all complexes of 1,4-diiodotetrafluorobenzene (other than hexane), the X−B bond lengths are less than 3.10 Å and R−X−B bond angles are greater than 173°. In our hexane control, E_{int} is very weakly favorable (−0.69 kJ/mol), and the interaction distance is 4.00 Å.

Comparison of Selectors. To better understand the dependence of the interaction energy on the nature of the halogen and EWGs, various selectors with RDX were compared (Table 1). The corresponding data for all analytes shown in Figure 1 can be found in the Supporting Information (Table SI-1). Using RDX as a representative example, we see that the interaction energy decreases from approximately −14 to −11 to −7 kJ/mol as the halogen changes from I to Br to Cl. Removal of the electron-withdrawing F atoms on the benzene ring of the selector results in a decrease in interaction energy with RDX of 3−4 kJ/mol (Table 1). For instance, the X−B interaction decreases if the iodine is substituted with bromine (diiodotetrafluorobenzene/RDX −13.93; dibromotetrafluorobenzene/RDX −11.33 kJ/mol) or with the removal of the fluorine EWGs (diiodotetrafluorobenzene/RDX −13.93; diiodobenzene/RDX −10.01 kJ/mol). The geometry optimized structure of 1,4-diiodotetrafluorobenzene with RDX (Figure 2C) demonstrates the structure of the halogen bonded complexes and the near linear dependence of the R−X−B bond angle. Structures for other complexes (Figures SI-1−SI-12) demonstrate the increase in X−B bond length when the electron withdrawing groups on the aromatic ring are not present and the X−B bond lengthens upon replacement of iodine with smaller halogens. In each case, the combination of removing EWGs and substituting another halogen for iodine results in a weakening of the X−B interaction. These trends hold true for all Lewis bases with all selectors included in this study (Supporting Information).

The electronic nature of the X−B bond acceptor plays a role in the structure and stability of these complexes. For instance, the aromatic explosive models would be expected to have less

Table 1. (Top) Computed Interaction Energies (kJ/mol) for Halogen-Bonded Complexes with Our Strongest Selector 1,4-Diiodotetrafluorobenzene and (Bottom) Interaction Energies (kJ/mol) for Halogen-Bonded Complexes with Nonaromatic Explosive RDX

	ΔE_{int} (kJ/mol)	X−B bond distance (Å)	R−X−B bond angle (θ)
Halogen-Bonded Complexes with Strongest Selector 1,4-Diiodotetrafluorobenzene			
model system			
NH_3	−37.18	2.86	179.9
aromatic explosives			
TNT	−15.14	3.10	173.9
2,4-DNT	−18.07	3.05	174.8
2,6-DNT	−17.77	3.07	173.8
nonaromatic explosives			
RDX	−13.93	3.10	174.9
HMX	−15.48	3.09	175.0
PETN	−16.75	3.27	162.5
taggant/byproduct			
CH	−23.42	2.89	179.1
DMNB	−18.22	3.04	173.6
nonbinder/control			
hexane	−0.69	4.00	168.9
Halogen-Bonded Complexes with Nonaromatic Explosive RDX			
1,4 diiodotetrafluorobenzene	−13.93	3.10	174.9
1,4 dibromotetrafluorobenzene	−11.33	3.04	174.1
1,4 dichlorotetrafluorobenzene	−7.09	3.11	172.1
1,4 diiodobenzene	−10.01	3.27	178.4
1,4 dibromobenzene	−7.85	3.20	176.6
1,4 dichlorobenzene	−4.33	3.24	174.0

DOI: 10.1021/acssensors.8b01246
ACS Sens. 2019, 4, 389−397

electron density on the oxygen atoms of the nitro groups due to resonance with the aromatic ring; however, the nonaromatic explosive models are attached to the ring via a nitrogen atom with a lone pair of electrons available for delocalization onto the nitro moiety. These competing electronic effects between aromatic and nonaromatic acceptors results in interaction energies that are within similar ranges. Molecules with greater conformational flexibility, such as HMX, PETN, and DMNB, form complexes with slightly longer X−B bond lengths (3.09, 3.27, and 3.04, respectively) while still maintaining favorable X−B interaction energies (−15.5, −16.8, and −18.2 kJ/mol, respectively). The especially long bond length in PETN complexes is driven by two stabilizing interactions: a halogen bond between the iodine on the sensor and a PETN NO_2 group and a secondary hydrogen-(diiodobenzene) or halogen-(diiodotetrafluorobenzene) bond with a neighboring PETN NO_2 group (Supporting Information, Figure SI-7).

The strength of the halogen bonded complexes reported here are not entirely unexpected given the theoretical work thus far and in accordance with X−B literature reports.[27−34,37,38,51,53−55] That is, X−B interaction is greatest with iodine as this is a larger, more easily polarized atom and most susceptible to nearby fluoride EWGs. These groups play a key role in pulling electrons away from X creating a larger area of positive electrostatic potential (sigma hole). However, in complexes with many conformational degrees of freedom and/or the possibility of steric interactions, optimal X−B bonding can be a complicated optimization of structural and electronic effects.[32]

For the purposes of eventually utilizing X−B for the detection of nonaromatic explosive molecules, the 1.21 kJ/mol difference in interaction energies between TNT (−13.93 kJ/mol) and RDX (−15.14 kJ/mol) with 1,4-diiodotetrafluorobenzene is particularly noteworthy, suggesting a clear and robust X−B interaction regardless of the aromaticity of the explosive molecule.

Using X−B Interactions for Detection of Explosive-Related Molecules. The development of sensing and biosensing devices that target molecules with specific intermolecular interactions such as H−B or X−B and using immobilized selectors often employ nanomaterials to increase surface area or enhance signal.[56] Sensors designed for the detection of explosives or explosive-related molecules are no exception to this trend. More recently, for example, Liu et al. showed that ethylenediamine-capped gold NPs could be used for the optical detection of TNT,[57] and Parkin and co-workers[58] demonstrated the use of quantum dots for the detection and differentiation of a number of explosives, including DNT, TNT, RDX, and PETN. A number of chemiresistive sensors for gas detection that feature nanomaterials have also been investigated, including work by Murray and Zamborini on NP film assemblies.[59] A major facet of this field of work is the employment of single-walled carbon nanotubes (SWCNTs) as their electronic properties allow them to be excellent reporters of changes in conductivity associated with molecules binding at their surface.[60] More specifically, work from the Swager lab on chemiresistive sensors with SWCNTs has produced some seminal reports targeting chemical warfare agents, including the use of covalently functionalized[24] and polymer-wrapped[25] SWCNTs as the basis of sensors targeting a nerve agent mimic and explosive-related molecules (i.e., cyclohexanone and nitromethane), respectively. Silane-modified films of SWCNT were also used by Swager and co-workers for sensors specifically targeting CH, a major component of the headspace above RDX.[26] Interestingly, a 2016 report from Swager[40] used SWCNTs modified with aryl-halide selector molecules to engage X−B interactions in the detection of pyridine and observed mixed results. To our knowledge, this current report is the first to experimentally employ X−B to specifically detect explosives or explosive-related molecules.

For the experimental portion of this study, the selector molecules identified computationally for their ability to engage in X−B were combined with SWCNTs in a chemiresistive sensor aimed at the detection of explosive-related molecules, including cyclohexanone (CH), a side-product of RDX production, and DMNB, a common taggant component in nonaromatic explosives (e.g., RDX, PETN). The p-SWCNTs were modified with the fluorinated and nonfluorinated halogen selectors as described in the Experimental Details section. The resulting composite material was compressed and mechanically drawn onto IDA electrodes[50] subsequently exposed to chemical vapor under amperometric monitoring at +0.1 V) (Figure 3). Interaction of the vapor molecules with the selectors at the SWCNTs should elicit a change in the conductivity of the film and a measurable current response such as the example shown in Figure 3B. As in numerous reports by Swager et al.,[24,25,50] normalized conductance of the film ($\Delta G/G$) can be derived from the current signal (see Additional Experimental Details, Supporting Information).

In order to establish X−B interactions as playing a major role in the sensing of CH, a series of SWCNT films were created with the various selector molecules: dihalides with and without the 2,3,5,6-tetrafluoro electron withdrawing groups as well as p-SWCNTs serving as a control. Each of these films were subjected to repeated exposures of 25, 50, or 75% CH vapor with nitrogen as the diluent alternated with 100% nitrogen flows. As shown in Figure 4 and summarized in the Supporting Information (Tables SI-2 and SI-3 and Figure SI-13), the change in conductance (normalized) and the response and recovery times were recorded for each of the films (Note: Raw data included as Supporting Information, Figures SI-14−SI-19). Each of the films responded to the CH vapor with signal that increased with increasing CH concentration, though the trend for the p-SWCNT control films was much more subtle compared to the robust response of films with selectors. The largest responses resulted from sensors with SWCNTs modified with either 1,4-diiodotetrafluorobenzene or 1,4-diiodobenzene with comparatively smaller responses recorded from their bromo-substituted counterparts. The data suggests that the presence of the iodine is more critical to the X−B interaction with CH than the presence of the electron withdrawing groups, a trend more easily seen by examining the average sensing response (Supporting Information, Figure SI-20). It is notable that the response time for all the selector films is similar (∼15−17 s) though slightly higher, on average, than that of the p-SWCNT control (∼9−10 s). In comparison, the recovery time after the film is returned to 100% nitrogen flow, while similar for the control film (∼11 s), is 3−4 times higher for the films with selector molecules (Supporting Information, Table SI-2). A comparison of amperometric $I-t$ responses for a p-SWCNT control film versus a film with the 1,4-diiodobenzene selector illustrates the longer recovery time of the selector film (Figure SI-21). This trend is to be expected if X−B is present, increasing the intermolecular forces that

DOI: 10.1021/acssensors.8b01246
ACS Sens. 2019, 4, 389−397

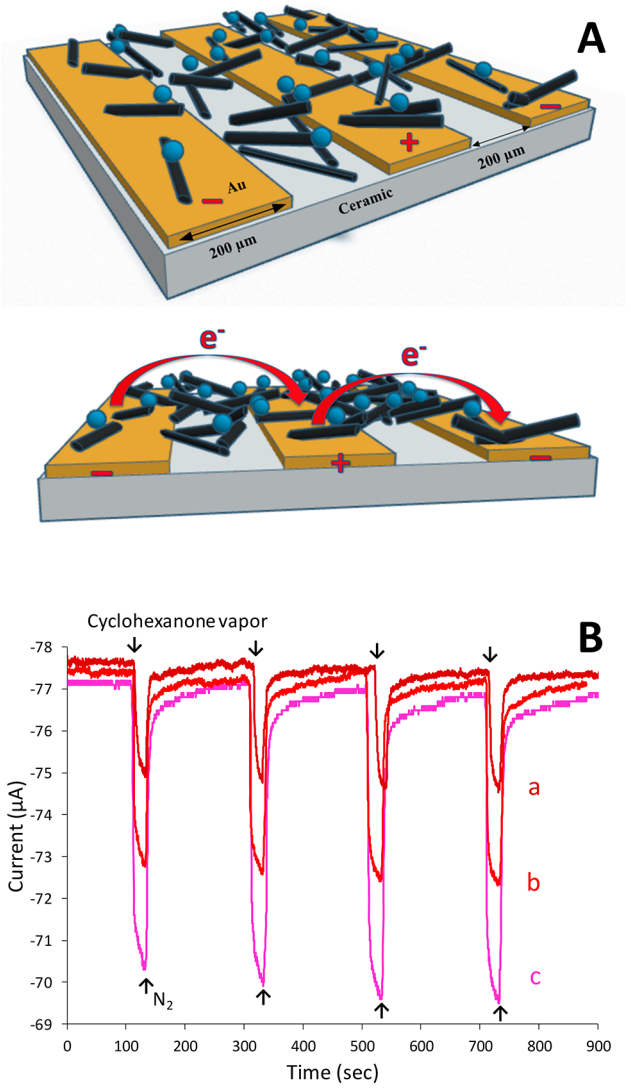

Figure 3. (A) Schematic overhead (top) and cross-sectional (bottom) representations of chemiresistive sensor comprised of randomly oriented p-SWCNTs modified with halogen bonding selector molecules deposited on an interdigitated array electrode (IDA) under applied potential; (B) typical amperiometric−time (I−t) curves collected at +0.1 V for p-SWCNTs modified with 1,4-diiodotetrafluorobenzene selector molecules exposed to a stream of nitrogen (↑) and vapor (↓) with (a) 25%, (b) 50%, and 75% cyclohexanone.

must be overcome before molecules desorb from the selector/SWCNT interface.

In order to confirm that the selectors were engaging in a major role in the interactions with CH molecules, additional SWCNT films featuring the 1,4-diiodotetrafluorobenzene selectors were prepared. In this set of experiments, films were prepared holding the mass of SWCNTs constant and increasing the concentration of 1,4-diiodotetrafluorobenzene selector, the hypothesis being that if the selector is critical to the CH interaction, a concentration dependent response should be observed. The results indicate that the conductance signal is dependent on the amount of 1,4-diiodotetrafluorobenzene selectors within the films, yielding a clear linear trend (Supporting Information, Figures SI-22−SI-26). An additional control experiment was conducted where a selector molecule unable to promote X−B interactions (octadecane) was incorporated with SWCNTs in order to differentiate the observed results from a simple film swelling mechanism. The prior study exploring X−B interactions for gas detection concluded film swelling was the predominant transduction mechanism.[40] Our results show that CNT films modified with octadecane resulted in conductance changes only moderately larger than the p-SWCNT control and smaller than all of the dihalogen selectors (Figures SI-13, SI-19, and SI-20). This suggests that X−B is significant in our selectors and plays a sizable role in the detection of CH. Additionally, the prior report showed X−B trends for pyridine detection with dihalogen substituted benzene selectors (i.e., I > Br > Cl) but was unsuccessful establishing the effect of electron-withdrawing groups predicted with X−B interactions (i.e., films with 1,4-diiodobenzene selectors yield a significantly higher pyridine interaction versus those with 1,4-diidodotetrafluorobenzene selectors).[40] In comparison, the current study targeting CH detection reveals both X−B trends are observable.

A CH concentration dependent response or linear calibration curve is easily attained when film assemblies with 1,4-diidodotetrafluorobenzene selectors are exposed to increasing relative concentrations of CH (% CH) in the nitrogen stream (Supporting Information, Figure SI-27). The response to CH is robust and extremely repeatable within a single sensor with relative standard error typically ≤2%. The device-to-device response is relatively repeatable with a typical relative of ∼15% given that each sensor is handmade, including mechanical abrasion of the SWCNT-selector composite material. The response toward CH is stable over time and responds to CH even after months of storing the films under ambient conditions (Figure SI-28).

A key component of any sensor development is selectivity, and while our film assemblies are still in a proof-of-concept stage of development, they were tested for selectivity against interferent species used in similar studies[26] and found in commonly used materials (e.g., perfume, fuels, smoke, nail polish, alcoholic beverages). The results, shown in Figure SI-29, suggest that the devices are exhibiting the same "class" selectivity toward compounds as observed in prior studies exploring X−B interactions of this kind for these targets. If the data is normalized for vapor pressure effects on concentration, an effect that can increase the vapor concentration by orders of magnitude,[26] the selectivity toward carbonyl class compounds like cyclohexanone is more pronounced (Figure SI-29). The selectivity results suggest that, analogous to prior studies with X−B, the films are exhibiting both inter-CNT swelling as well as intra-CNT dipole interactions with the carbonyl group of CH that affects cationic carriers or holes within the film.[22,26] We suspect that the selectivity responses may have a higher influence of swelling effects than prior studies as we are currently unable to achieve similar low concentration levels with our apparatus.[26] Improving the discrimination of the response toward more specific selectivity remains a goal of the next stage of these studies.

The established X−B based detection of CH at the SWCNT/1,4-diidootetrafluorobenzene composite films prompted an attempt to use the same system to detect DMNB, a common taggant added to a number of nonaromatic explosives. Unlike CH, a volatile liquid that is easily converted to vapor in a flow system, DMNB, like the nonaromatic explosives, is significantly less volatile and must first be dissolved in a solvent, in this case, acetonitrile. Given its low vapor pressure, the response of DMNB at the sensors is

DOI: 10.1021/acssensors.8b01246
ACS Sens. 2019, 4, 389−397

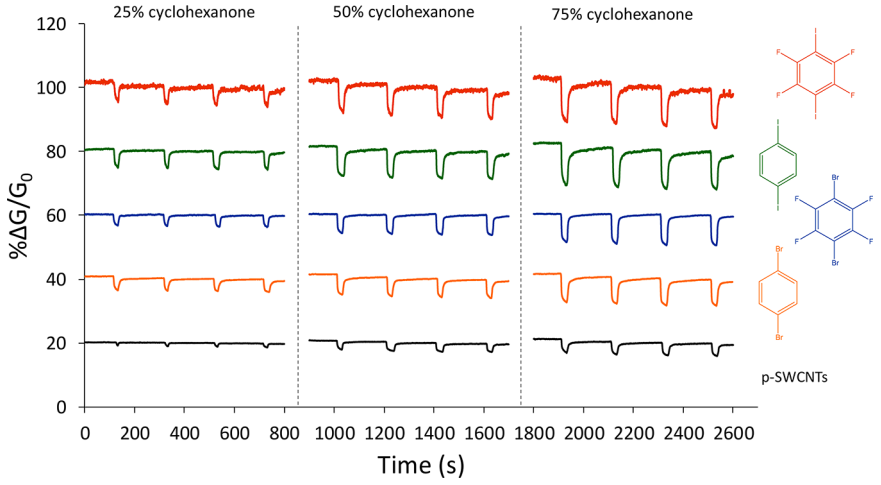

Figure 4. Sensing response of normalized conductive change [$\Delta G/G$ (%)] of SWCNT-based sensors with various selector molecules (right) when exposed to vapor with varying concentrations of cyclohexanone (CH). For clarity, each series is displayed with a 20% offset. Normalization/baseline correction procedure is described in more detail in the Supporting Information.

expected to be smaller than prior results and must be compared to controls of p-SWCNT films as well as exposure to acetonitrile vapor. The difference in response for SWCNT control films toward the acetonitrile vapor versus the DMNB saturated acetonitrile vapor is negligible (with % $\Delta G/G$ values of 2.46 (±0.10) vs 2.41 (±0.02), respectively. The same exposures at the SWCNT/1,4-diidootetrafluorobenzene films show a small but consistent increased response when DMNB is present with $\Delta G/G$ values of 2.78 (±0.34)% vs 3.77 (±0.45), results suggesting that X−B may be present between the selectors and the target molecule (Figure SI-30). These preliminary results with DMNB, while promising, clearly prompt the development of a more sophisticated flow system able to vaporize DMNB without solvent (e.g., permeation tubes) before definitive conclusions can be made for X−B-based detection using these films. An additional optimization of the flow system that may elicit an even more sensitive response in these systems is the use of a different carrier gas where, using the same theoretical modeling, the E_{int} between Ar and N_2 with 1,4-diiodotetrafluorobenzene was small, i.e., −0.51 and −4.98 kJ/mol, respectively. While this result implies very little screening on the part of the carrier gas, it suggests that stronger experimental results may be achieved with the use of argon in future experiments.

CONCLUSIONS

Computationally, dihalobenzene-based selector molecules form favorable, halogen bonding interactions with aromatic and nonaromatic explosives as well as with byproduct CH and taggant DMNB. In all cases, the complexes contain interaction distances less than 3.4 Å and with R−X−B bond angles ranging between 160 and 180°. Computationally, the diiodotetrafluorobenzene selector formed the most favorable halogen-bonded structures, in agreement with our experimental results. Experimentally, a sensing device was fabricated and the detection of CH and DMNB was demonstrated. Results suggest that the sensing mechanism is based on halogen bonding interactions and that the presence of iodine in the selector is critical to its effectiveness.

ASSOCIATED CONTENT

Supporting Information

The Supporting Information is available free of charge on the ACS Publications website at DOI: 10.1021/acssensors.8b01246.

Additional experimental details, computational results (interaction energies, X−B bond lengths and angles), amperometric $I-t$ curves, film resistances, sensing performance data summary tables for most films and selector combinations, selector and CH concentration dependence, selectivity assessment, and DMNB results (PDF)

AUTHOR INFORMATION

Corresponding Authors

*E-mail: mleopold@richmond.edu. Phone: (804) 287-6329.
*E-mail: cparish@richmond.edu. Phone: (804) 484-1548.

ORCID

Carol A. Parish: 0000-0003-2878-3070

Funding

The research was generously supported by the NSF (Grant CHE-1401593, M.C.L. and Grants CHE-1800014 and CHE-1213271, C.A.P.), Department of Energy (Grant DE-SC0001093, C.A.P.) and Donors of the ACS-PRF (C.A.P.), as well as the Arnold and Mabel Beckman Foundation (A.K.A.J.), the Camille & Henry Dreyfus Foundation (M.C.L.), and the Floyd D. and Elisabeth S. Gottwald Endowed Chair of Chemistry (M.C.L.). Computational resources were provided, in part, by the MERCURY supercomputer consortium under NSF Grant CHE-1626238.

Notes

The authors declare no competing financial interest.

ACKNOWLEDGMENTS

We would like to thank Ken and Sally Hughes at K&S Tool & Mfg. Co. for construction of the our cell housing design for the sensor array and Dr. Carrie Wu (University of Richmond Biology Department) for use of the ball-miller.

DOI: 10.1021/acssensors.8b01246
ACS Sens. 2019, 4, 389−397

REFERENCES

(1) Senesac, L.; Thundat, T. G. Nanosensors for trace explosive detection. *Mater. Today* **2008**, *11* (3), 28−36.
(2) Lai, H.; Leung, A.; Magee, M.; Almirall, J. R. Identification of volatile chemical signatures from plastic explosives by SPME-GC/MS and detection by ion mobility spectrometry. *Anal. Bioanal. Chem.* **2010**, *396*, 2997−3007.
(3) Furton, K. G.; Myers, L. J. The scientific foundation and efficacy of the use of canines as chemical detectors for explosives1Invited paper for the special issue of Talanta 'Methods for Explosive Analysis and Detection'.1. *Talanta* **2001**, *54* (3), 487−500.
(4) Stancl, M. Detection of Traces of Explosives by Means of Sniffing Dogs. In *Vapour and Trace Detection of Explosives for Anti-Terrorism Purposes*; Krausa, M., Ed. Springer: Dordrecht, The Netherlands, 2004; Vol. *167*.
(5) Ewing, R. G.; Atkinson, D. A.; Eiceman, G. A.; Ewing, G. J. A critical review of ion mobility spectrometry for the detection of explosives and explosive related compounds. *Talanta* **2001**, *54* (3), 515−529.
(6) Ewing, R. G.; Miller, C. J. Detection of volatile vapors emitted from explosives with a handheld ion mobility spectrometer. *Field Anal. Chem. Technol.* **2001**, *5* (5), 215−221.
(7) Germain, M. E.; Knapp, M. J. Optical explosives detection: from color changes to fluorescence turn-on. *Chem. Soc. Rev.* **2009**, *38* (9), 2543−2555.
(8) Gares, K. L.; Hufziger, K. T.; Bykov, S. V.; Asher, S. A. Review of explosive detection methodologies and the emergence of standoff deep UV resonance Raman. *J. Raman Spectrosc.* **2016**, *47*, 124−141.
(9) Pamula, V. K.; Srinivasan, V.; Chakrapani, H.; Fair, R. B.; Toone, E. J.A droplet-based lab-on-a-chip for colorimetric detection of nitroaromatic explosives. In *18th IEEE International Conference on Micro Electro Mechanical Systems, 2005. MEMS 2005*, January 30−3 February 3, 2005; pp 722−725.
(10) Liu, Y.; Mills, R. C.; Boncella, J. M.; Schanze, K. S. Fluorescent Polyacetylene Thin Film Sensor for Nitroaromatics. *Langmuir* **2001**, *17* (24), 7452−7455.
(11) Rochat, S.; Swager, T. M. Conjugated Amplifying Polymers for Optical Sensing Applications. *ACS Appl. Mater. Interfaces* **2013**, *5* (11), 4488−4502.
(12) Swager, T. M. The Molecular Wire Approach to Sensory Signal Amplification. *Acc. Chem. Res.* **1998**, *31* (5), 201−207.
(13) Thomas, S. W.; Joly, G. D.; Swager, T. M. Chemical Sensors Based on Amplifying Fluorescent Conjugated Polymers. *Chem. Rev.* **2007**, *107* (4), 1339−1386.
(14) Yan, J.; Ni, J. C.; Zhao, J. X.; Sun, L. X.; Bai, F. Y.; Shi, Z.; Xing, Y. H. The nitro aromatic compounds detection by triazole carboxylic acid and its complex with the fluorescent property. *Tetrahedron* **2017**, *73* (18), 2682−2689.
(15) Yang, J.-S.; Swager, T. M. Fluorescent Porous Polymer Films as TNT Chemosensors: Electronic and Structural Effects. *J. Am. Chem. Soc.* **1998**, *120* (46), 11864−11873.
(16) Andrew, T. L.; Swager, T. M. A Fluorescence Turn-On Mechanism to Detect High Explosives RDX and PETN. *J. Am. Chem. Soc.* **2007**, *129* (23), 7254−7255.
(17) Germain, M. E.; Knapp, M. J. Turn-on Fluorescence Detection of H_2O_2 and TATP. *Inorg. Chem.* **2008**, *47* (21), 9748−9750.
(18) Swager, T. M.; Wosnick, J. H. Self-Amplifying Semiconducting Polymers for Chemical Sensors. *MRS Bull.* **2002**, *27* (6), 446−450.
(19) Xia, Y.; Song, L.; Zhu, C. Turn-On and Near-Infrared Fluorescent Sensing for 2,4,6-Trinitrotoluene Based on Hybrid (Gold Nanorod)−(Quantum Dots) Assembly. *Anal. Chem.* **2011**, *83* (4), 1401−1407.
(20) Cumming, C. J.; Aker, C.; Fisher, M.; Fok, M.; Grone, M. J. l.; Reust, D.; Rockley, M. G.; Swager, T. M.; Towers, E.; Williams, V. Using novel fluorescent polymers as sensory materials for above-ground sensing of chemical signature compounds emanating from buried landmines. *IEEE Transactions on Geoscience and Remote Sensing* **2001**, *39* (6), 1119−1128.
(21) Andrew, T. L.; Swager, T. M. Detection of explosives via photolytic cleavage of nitroesters and nitramines. *J. Org. Chem.* **2011**, *76* (9), 2976−93.
(22) Schroeder, V.; Savagatrup, S.; He, M.; Lin, S.; Swager, T. M. Carbon Nanotube Chemical Sensors. *Chem. Rev.* **2019**, *119*, 599−663.
(23) Schnorr, J. M.; Swager, T. M. Emerging Applications of Carbon Nanotubes. *Chem. Mater.* **2011**, *23* (3), 646−657.
(24) Schnorr, J. M.; Van der Zwaag, D.; Walish, J. J.; Weizmann, Y.; Swager, T. M. Sensory Arrays of Covalently Functionalized Single-Walled Carbon Nanotubes for Explosive Detection. *Adv. Funct. Mater.* **2013**, *23* (42), 5285−5291.
(25) Fennell, J.; Hamaguchi, H.; Yoon, B.; Swager, T. Chemiresistor Devices for Chemical Warfare Agent Detection Based on Polymer Wrapped Single-Walled Carbon Nanotubes. *Sensors* **2017**, *17* (5), 982.
(26) Frazier, K. M.; Swager, T. M. Robust cyclohexanone selective chemiresistors based on single-walled carbon nanotubes. *Anal. Chem.* **2013**, *85* (15), 7154−8.
(27) Cavallo, G.; Metrangolo, P.; Milani, R.; Pilati, T.; Priimagi, A.; Resnati, G.; Terraneo, G. The Halogen Bond. *Chem. Rev.* **2016**, *116* (4), 2478−2601.
(28) Politzer, P.; Murray, J. S.; Clark, T. Halogen bonding: an electrostatically-driven highly directional noncovalent interaction. *Phys. Chem. Chem. Phys.* **2010**, *12* (28), 7748−57.
(29) Clark, T.; Hennemann, M.; Murray, J. S.; Politzer, P. Halogen bonding: the σ-hole. *J. Mol. Model.* **2007**, *13* (2), 291−296.
(30) Donald, K. J.; Wittmaack, B. K.; Crigger, C. Tuning σ-Holes: Charge Redistribution in the Heavy (Group 14) Analogues of Simple and Mixed Halomethanes Can Impose Strong Propensities for Halogen Bonding. *J. Phys. Chem. A* **2010**, *114*, 7213−7222.
(31) Donald, K. J.; Tawfik, M. The Weak Helps the Strong: Sigma-Holes and the Stability of MF4·Base Complexes. *J. Phys. Chem. A* **2013**, *117*, 14176−14183.
(32) Parker, A. J.; Stewart, J.; Donald, K. J.; Parish, C. A. Halogen bonding in DNA base pairs. *J. Am. Chem. Soc.* **2012**, *134* (11), 5165−72.
(33) Shirman, T.; Kaminker, R.; Freeman, D.; Van der Boom, M. E. Halogen-Bonding Mediated Stepwise Assembly of Gold Nanoparticles onto Planar Surfaces. *ACS Nano* **2011**, *5* (8), 6553−6563.
(34) Metrangolo, P.; Neukirch, H.; Pilati, T.; Resnati, G. Halogen Bonding Based Recognition Processes: A World Parallel to Hydrogen Bonding. *Acc. Chem. Res.* **2005**, *38*, 386−395.
(35) Zhu, S.; Xing, C.; Xu, W.; Jin, G.; Li, Z. Halogen Bonding and Hydrogen Bonding Coexist in Driving Self-Assembly Process. *Cryst. Growth Des.* **2004**, *4* (1), 53−56.
(36) Zapata, F.; Benitez-Benitez, S. J.; Sabater, P.; Caballero, A.; Molina, P. Modulation of the selectivity in anions recognition processes by combining hydrogen- and halogen-bonding interactions. *Molecules* **2017**, *22*, 2273−2273.
(37) Guo, N.; Maurice, R.; Teze, D.; Graton, J.; Champion, J.; Montavon, G.; Galland, N. Experimental and computational evidence of halogen bonds involving astatine. *Nat. Chem.* **2018**, *10* (4), 428−434.
(38) Langton, M. J.; Marques, I.; Robinson, S. W.; Felix, V.; Beer, P. D. Iodide Recognition and Sensing in Water by a Halogen-Bonding Ruthenium(II)-Based Rotaxane. *Chem. - Eur. J.* **2016**, *22*, 185−192.
(39) Lim, J. Y. C.; Marques, I.; Ferreira, L.; Felix, V.; Beer, P. D. Enhancing the enantioselective recognition and sensing of chiral anions by halogen bonding. *Chem. Commun. (Cambridge, U. K.)* **2016**, *52*, 5527−5530.
(40) Weis, J. G.; Ravnsbæk, J. B.; Mirica, K. A.; Swager, T. M. Employing Halogen Bonding Interactions in Chemiresistive Gas Sensors. *ACS Sensors* **2016**, *1* (2), 115−119.
(41) Mullaney, B. R.; Cunningham, M. J.; Davis, J. J.; Beer, P. D. Acyclic halogen and hydrogen bonding diquat-containing receptors for the electrochemical sensing of anions. *Polyhedron* **2016**, *116*, 20−25.

DOI: 10.1021/acssensors.8b01246
ACS Sens. 2019, 4, 389−397

(42) Gale, P. A.; Caltagirone, C. Fluorescent and colorimetric sensors for anionic species. *Coord. Chem. Rev.* **2018**, *354*, 2−27.
(43) Frisch, M. J.; Trucks, G. W.; Schlegel, H. B.; Scuseria, G. E.; Robb, M. A.; Cheeseman, J. R.; Scalmani, G.; Barone, V.; Mennucci, B.; Petersson, G. A.; Nakatsuji, H.; Caricato, M.; Li, X.; Hratchian, H. P.; Izmaylov, A. F.; Bloino, J.; Zheng, G.; Sonnenberg, J. L.; Hada, M.; Ehara, M.; Toyota, K.; Fukuda, R.; Hasegawa, J.; Ishida, M.; Nakajima, T.; Honda, Y.; Kitao, O.; Nakai, H.; Vreven, T.; Montgomery, J. A., Jr.; Peralta, J. E.; Ogliaro, F.; Bearpark, M.; Heyd, J. J.; Brothers, E.; Kudin, K. N.; Staroverov, V. N.; Kobayashi, R.; Normand, J.; Raghavachari, K.; Rendell, A.; Burant, J. C.; Iyengar, S. S.; Tomasi, J.; Cossi, M.; Rega, N.; Millam, J. M.; Klene, M.; Knox, J. E.; Cross, J. B.; Bakken, V.; Adamo, C.; Jaramillo, J.; Gomperts, R.; Stratmann, R. E.; Yazyev, O.; Austin, A. J.; Cammi, R.; Pomelli, C.; Ochterski, J. W.; Martin, R. L.; Morokuma, K.; Zakrzewski, V. G.; Voth, G. A.; Salvador, P.; Dannenberg, J. J.; Dapprich, S.; Daniels, A. D.; Farkas, Ö.; Foresman, J. B.; Ortiz, J. V.; Cioslowski, J.; Fox, D. J. *Gaussian 09*, revision E.01; Gaussian, Inc.: Wallingford CT, 2009.
(44) Stephens, P. J.; Devlin, F. J.; Chabalowski, C. F.; Frisch, M. J. Ab Initio Calculation of Vibrational Absorption and Circular Dichroism Spectra Using Density Functional Force Fields. *J. Phys. Chem.* **1994**, *98* (45), 11623−11627.
(45) Dunning, T. H. J. Gaussian-basis sets for use in correlated molecular calculations. I. The atoms boron through neon and hydrogen. *J. Chem. Phys.* **1989**, *90* (2), 1007.
(46) Woon, D. E., Jr.; Dunning, T. H. Gaussian basis sets for use in correlated molecular calculations. III. The atoms aluminum through argon. *J. Chem. Phys.* **1993**, *98* (2), 1358−1371.
(47) Stoll, H.; Metz, B.; Dolg, M. Relativistic energy-consistent pseudopotentials—Recent developments. *J. Comput. Chem.* **2002**, *23* (8), 767−778.
(48) Peterson, K. A.; Shepler, B. C.; Figgen, D.; Stoll, H. On the Spectroscopic and Thermochemical Properties of ClO, BrO, IO, and Their Anions. *J. Phys. Chem. A* **2006**, *110* (51), 13877−13883.
(49) Mirica, K. A.; Azzarelli, J. M.; Weis, J. G.; Schnorr, J. M.; Swager, T. M. Rapid prototyping of carbon-based chemiresistive gas sensors on paper. *Proc. Natl. Acad. Sci. U. S. A.* **2013**, *110* (35), E3265−70.
(50) Mirica, K. A.; Weis, J. G.; Schnorr, J. M.; Esser, B.; Swager, T. M. Mechanical Drawing of Gas Sensors on Paper. *Angew. Chem., Int. Ed.* **2012**, *51* (43), 10740−10745.
(51) Tawfik, M.; Donald, K. J. Halogen Bonding: Unifying Perspectives on Organic and Inorganic Cases. *J. Phys. Chem. A* **2014**, *118*, 10090−10100.
(52) Wendler, K.; Thar, J.; Zahn, S.; Kirchner, B. Estimating the Hydrogen Bond Energy. *J. Phys. Chem. A* **2010**, *114* (35), 9529−9536.
(53) Politzer, P.; Murray, J. S.; Clark, T. Halogen bonding: an electrostatically-driven highly directional noncovalent interaction. *Phys. Chem. Chem. Phys.* **2010**, *12* (28), 7748−7757.
(54) Solimannejad, M.; Malekani, M.; Alkorta, I. Substituent Effects on the Cooperativity of Halogen Bonding. *J. Phys. Chem. A* **2013**, *117* (26), 5551−5557.
(55) Su, M.-D.; Chu, S.-Y. Reactivity of the C−X (X = F, Cl, Br, and I) Bond Activation in CX4 by an Iridium(I) Complex from a Theoretical Viewpoint. *J. Am. Chem. Soc.* **1999**, *121* (5), 1045−1058.
(56) Zhu, C.; Yang, G.; Li, H.; Du, D.; Lin, Y. Electrochemical Sensors and Biosensors Based on Nanomaterials and Nanostructures. *Anal. Chem.* **2015**, *87* (1), 230−249.
(57) Lin, D.; Liu, H.; Qian, K.; Zhou, X.; Yang, L.; Liu, J. Ultrasensitive optical detection of trinitrotoluene by ethylenediamine-capped gold nanoparticles. *Anal. Chim. Acta* **2012**, *744*, 92−98.
(58) Peveler, W. J.; Roldan, A.; Hollingsworth, N.; Porter, M. J.; Parkin, I. P. Multichannel Detection and Differentiation of Explosives with a Quantum Dot Array. *ACS Nano* **2016**, *10* (1), 1139−1146.
(59) Zamborini, F. P.; Leopold, M. C.; Hicks, J. F.; Kulesza, P. J.; Malik, M. A.; Murray, R. W. Electron Hopping Conductivity and Vapor Sensing Properties of Flexible Network Polymer Films of Metal Nanoparticles. *J. Am. Chem. Soc.* **2002**, *124* (30), 8958−8964.
(60) Wang, J. Carbon-Nanotube Based Electrochemical Biosensors: A Review. *Electroanalysis* **2005**, *17* (1), 7−14.

DOI: 10.1021/acssensors.8b01246
ACS Sens. 2019, 4, 389−397